

**Enzymatically degradable nitric oxide releasing *S*-nitrosated dextran thiomers for  
biomedical applications**

Vinod B. Damodaran,<sup>a</sup> Laura W. Place,<sup>b</sup> Matt J. Kipper<sup>b,c</sup> and  
Melissa M. Reynolds<sup>a,b,\*</sup>

<sup>a</sup>Department of Chemistry, <sup>b</sup>School of Biomedical Engineering, and <sup>c</sup>Department of Chemical  
and Biological Engineering and, Colorado State University, Fort Collins, CO 80523, USA.

\*Corresponding author

Tel: +1 970 491 3775

e-mail: melissa.reynolds@colostate.edu

<b>S. No</b>	<b>Content</b>	<b>Page No</b>
1	FTIR-ATR spectrum of <i>S</i> -nitrosated dextran-cysteamine	S3
2	FTIR-ATR spectra of dextran, CM-dextran, dextran-cysteine and <i>S</i> -nitrosated dextran-cysteine	S4
3	Representative UV absorption spectrum of <i>S</i> -nitrosated dextran-cysteine against dextran-cysteine baseline	S5
4	Stabilization of <i>S</i> -nitrosated dextran derivatives	S6
5	Summary of NO recovery under acidic and thermal, dry conditions over extended period	S7
6	Representative real-time NO release profile from <i>S</i> -nitrosated dextran derivatives under acidic conditions	S8
7	Representative total NO release curves for <i>S</i> -nitrosated dextran derivatives under acidic conditions	S9
8	Representative real-time NO release profile from <i>S</i> -nitrosated dextran derivatives under thermal dry conditions	S10
9	Representative total NO release curves for <i>S</i> -nitrosated dextran derivatives under thermal dry conditions	S11
10	Model for polymer degradation and representative GPC data for degradation of dextran-cysteamine and dextran-cysteamine SNO	S12-S16
11	References	S17

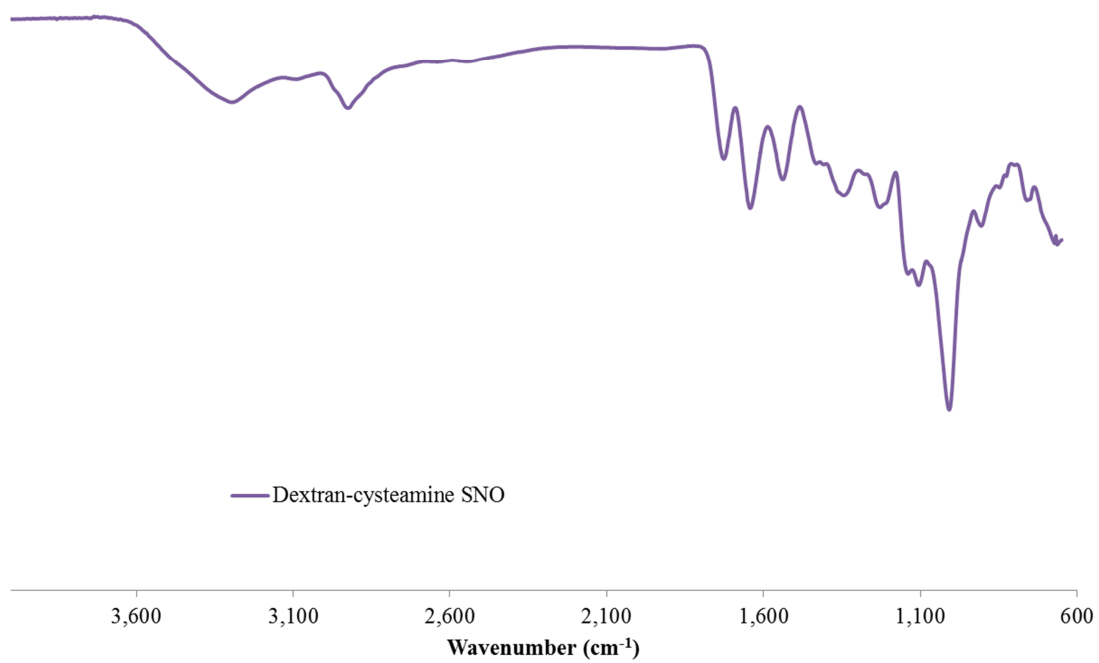


**Figure S1** FTIR-ATR spectrum of *S*-nitrosated dextran-cysteamine

*Electronic Supplementary Information*

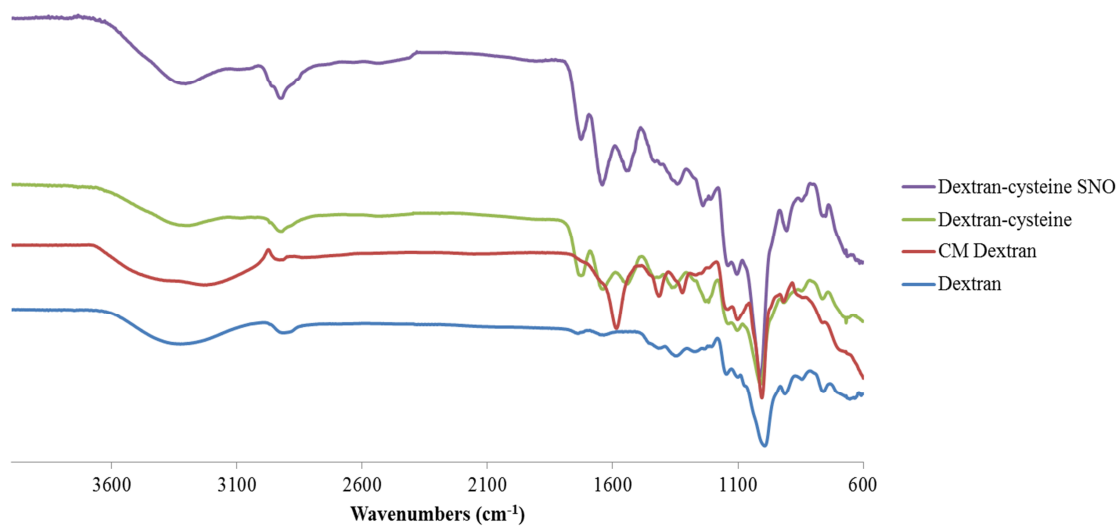


**Figure S2** FTIR-ATR spectra of dextran, CM-dextran, dextran-cysteine and *S*-nitrosated dextran-cysteine

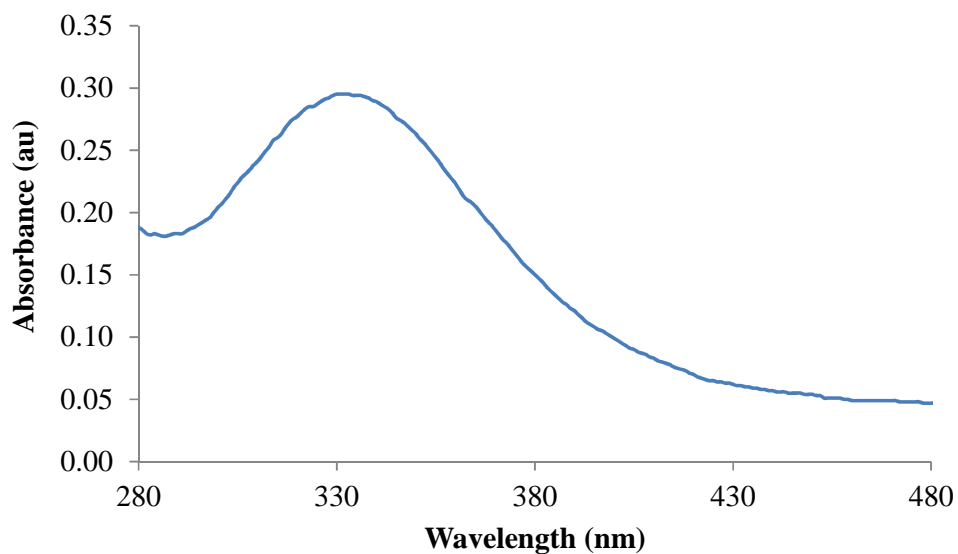
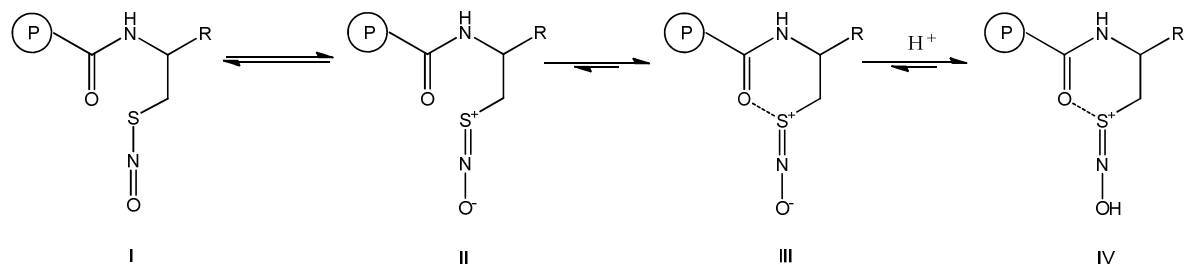


**Figure S3** Representative UV absorption spectrum of *S*-nitrosated dextran-cysteine (1.5 mg/mL in DI water) against dextran-cysteine baseline (1.5 mg/mL in DI water)

### Stabilization of *S*-nitrosated dextran derivatives



where R = H for cysteamine and COOH for cysteine

**Figure S4** *S*-nitrosated dextran derivatives reported herein stabilized through the formation of a stable six membered intermediate and through the formation of partial double bond nature of the S-N bond (intermediates II and III)<sup>1</sup>. Under acidic conditions, the intermediate III further stabilized through the formation of an *N*-hydroxyl derivative (intermediate IV).

**Table S1** Summary of NO recovery under acidic and thermal, dry conditions over extended period<sup>‡</sup>

<i>S</i> -nitrosated dextran derivative	Acidic (50 mM citrate buffer/pH 5/ 37 °C/72 h)*		Thermal, dry (Step-wise heating up to 100 °C) <sup>#</sup>	
	% NO		% NO	
	mmol NO /g	recovery based on SNO	mmol NO /g	recovery based on SNO
Dex-cysteamine SNO	0.082 ± 0.001	39.8 ± 0.7	0.180 ± 0.006	88.1 ± 2.7
Dex-cysteine SNO	0.091 ± 0.013	52.5 ± 7.2	0.166 ± 0.005	95.3 ± 2.6

Notes: <sup>‡</sup>Uncertainties represent standard deviation from multiple experiments (n > 3)

\*Both the materials were found to release NO above baseline even after 72h.

<sup>#</sup>See Fig. S7 and S8 for the heating profile and release kinetics.

Electronic Supplementary Information

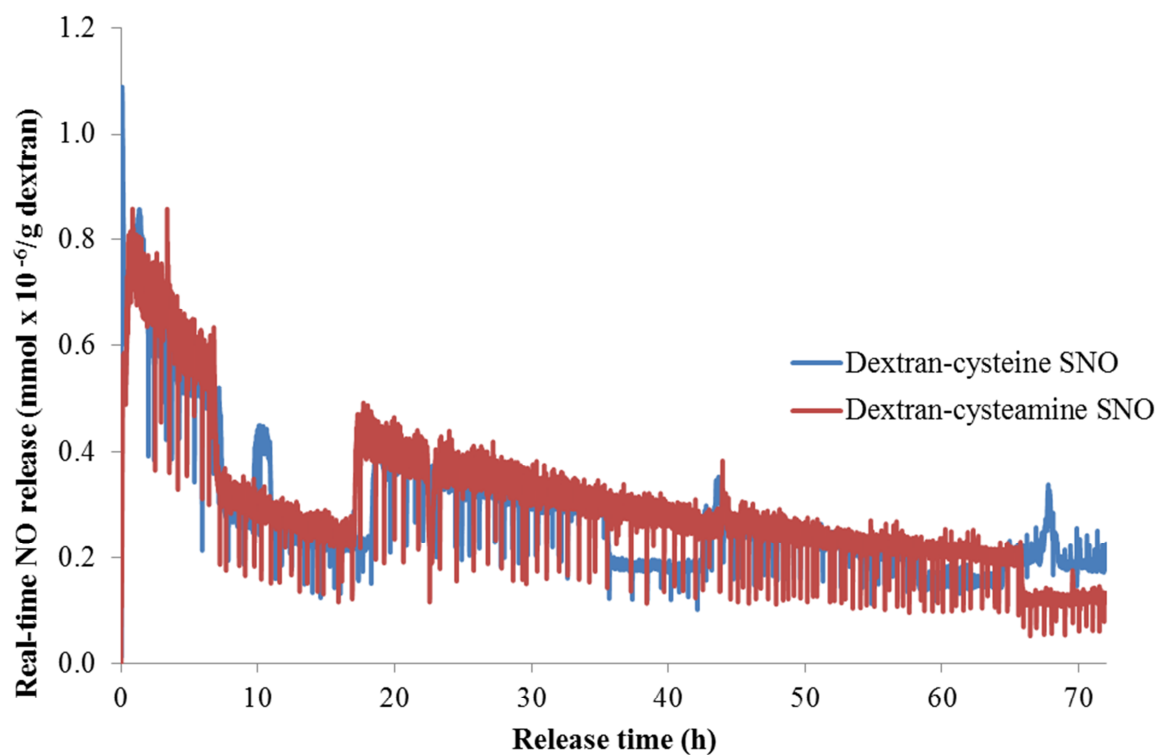


**Figure S5** Representative real-time NO release profile from *S*-nitrosated dextran derivatives under acidic conditions (50 mM citrate buffer/pH 5/ 37 °C/72 h) (n > 3).



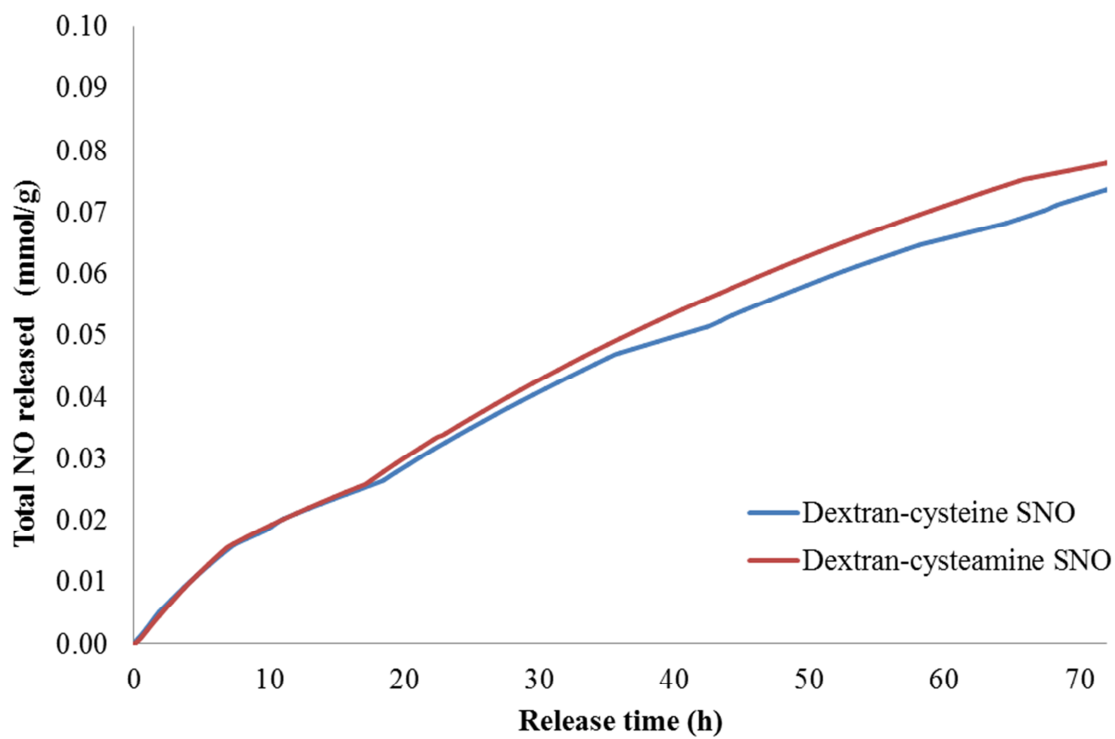


**Figure S6** Representative total NO release curves for *S*-nitrosated dextran derivatives under acidic conditions (50 mM citrate buffer/pH 5/ 37 °C/72 h) (n > 3)

Electronic Supplementary Information

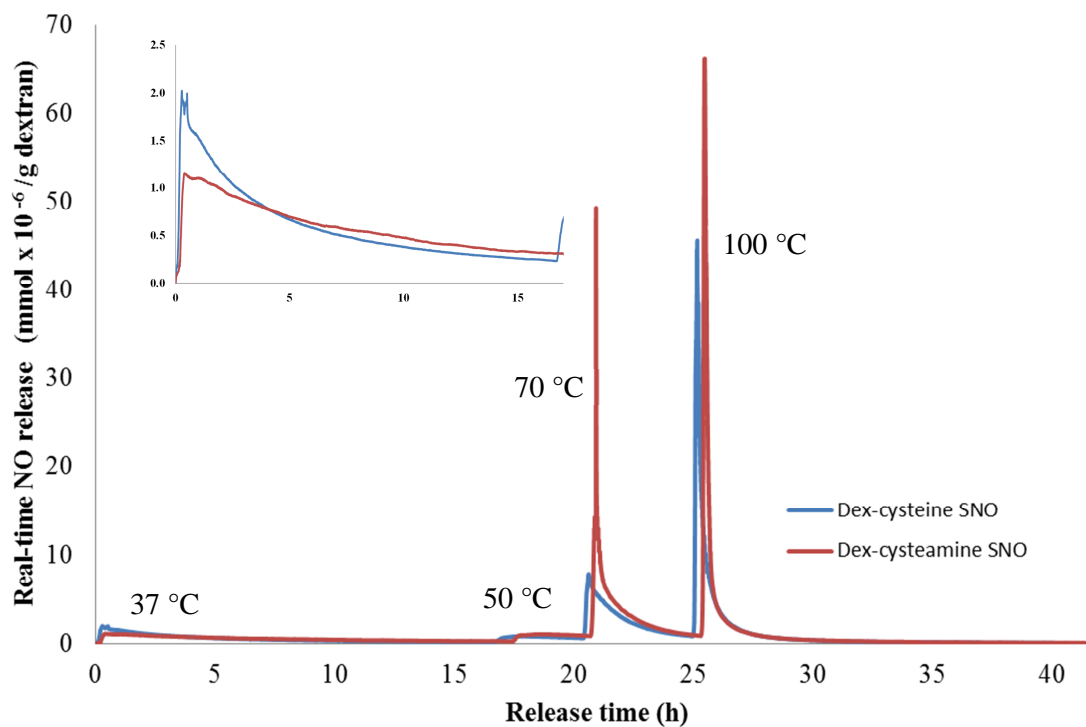


**Figure S7** Representative real-time NO release profile from *S*-nitrosated dextran derivatives under thermal dry conditions (Step-wise heating up to 100 °C) ( $n > 3$ ). Insert figure shows an expanded version of the same figure for the initial 17 h showing NO release at 37 °C above the baseline.

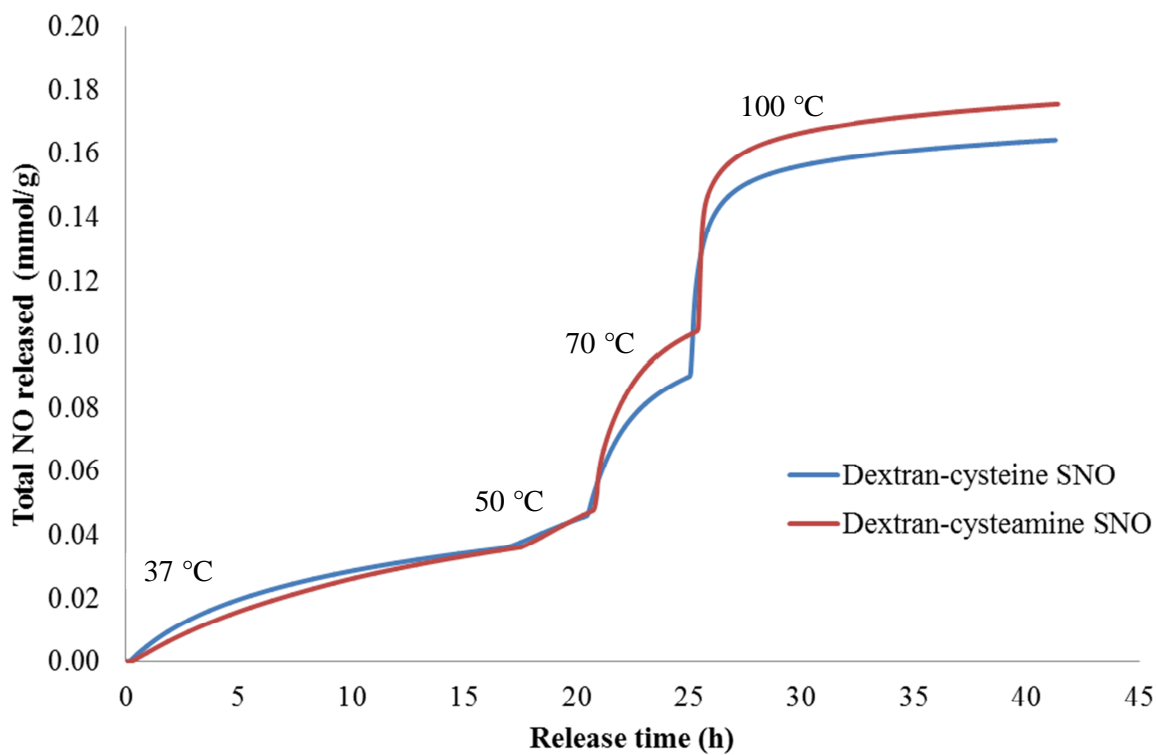
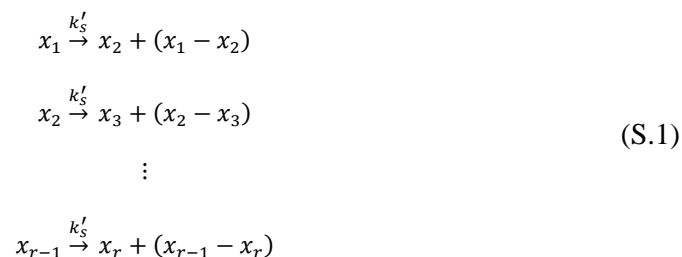


**Figure S8** Representative total NO release curves for *S*-nitrosated dextran derivatives under thermal dry conditions (Step-wise heating up to 100 °C) ( $n > 3$ )

### Model for polymer degradation and representative GPC data for degradation of dextran-cysteamine and dextran-cysteamine SNO

McCoy and Madras show that when a polydisperse polymer with a molecular weight distribution (MWD) approximated by a gamma distribution degrades by random chain scission, the products of degradation also have gamma distributions.<sup>2</sup> This readily enables the use of a moment analysis to describe the MWD of the degrading polymer. The sequential degradation of a single polymer chain of molecular weight  $x_1$  to products of molecular weights  $x_2, x_3, \dots$  and  $x_r$  occurs by a series of  $r - 1$  reactions in series



McCoy and Madras assume that degradation is first order in polymer concentration.<sup>2</sup> In reactions S.1 we denote an apparent pseudo first order rate coefficient for the enzymatic degradation, approximated as  $k'_s = k_s[E]$ , where  $k_s$  is the second order rate coefficient and  $[E]$  is the total enzyme concentration. This assumes that the rate is independent of the reactant polymer molecular weight, and that the enzyme primarily exists as free enzyme in solution.

McCoy and Madras show that for a batch reaction, the  $n^{\text{th}}$  moment of the reactant polymer MWD,  $p_1^{(n)}$ , and the product polymer MWDs,  $p_2^{(n)}, p_3^{(n)}, \dots$  and  $p_r^{(n)}$ , corresponding to the 2, 3, ... and  $r$  product generations evolve according to

$$\frac{dp_1^{(n)}}{dt} = -k'_s p_1^{(n)}\tag{S.2}$$

$$\frac{dp_i^{(n)}}{dt} = -k'_s p_i^{(n)} + 2Z_n k'_s p_{i-1}^{(n)}; \quad \text{for } 1 < i < r$$

$$\frac{dp_r^{(n)}}{dt} = 2Z_n k'_s p_{r-1}^{(n)}$$

$Z_n$  is a constant that depends upon the probability of scission occurring at different points in the polymer chain. For random chain scission,  $Z_n = 1/(1 + n)$ . Equations S.2 can be integrated sequentially using the initial conditions

$$\begin{aligned} p_1^{(n)}(t = 0) &= p_0^{(n)} \\ p_i^{(n)}(t = 0) &= 0; \quad \text{for } 1 < i \end{aligned} \quad (\text{S.3})$$

The transient solutions are

$$\begin{aligned} p_1^{(n)} &= p_0^{(n)} e^{-k'_s t} \\ p_i^{(n)} &= \frac{(2k'_s Z_n t)^{i-1}}{(i-1)!} p_0^{(n)} e^{-k'_s t}; \quad \text{for } 1 < i < r \\ p_r^{(n)} &= (2k'_s Z_n)^{r-1} p_0^{(n)} \left[ 1 - \sum_{j=0}^{r-2} \frac{(k'_s t)^j}{j!} e^{-k'_s t} \right] \end{aligned} \quad (\text{S.4})$$

For the general case, the  $n^{\text{th}}$  moment of the complete MWD, is the sum of moments of the reactant polymer and all individual degradation products

$$p^{(n)} = \sum_{i=1}^r p_i^{(n)} \quad (\text{S.5})$$

This is the solution presented by McCoy and Madras.<sup>2</sup> For equations S.4, the summation in equation S.5 becomes equation 1 in the main text. Equation 1 was used in this work to model the degradation of the dextran-cysteine SNO and the dextran-cysteamine SNO, with  $r = 5$  and  $r = 4$ , respectively. Representative refractive index and light scattering traces from GPC of the dextran-cysteine SNO, and a fit of equation 3 to the  $M_w(t)$  data is shown in Fig. 8 of the main text. Figure S8 below shows similar data for the dextran-cysteamine SNO degradation experiment. The  $M_w(t)$  data for  $t = 6$  hours to  $t = 120$  are used to obtain the fit

Electronic Supplementary Information

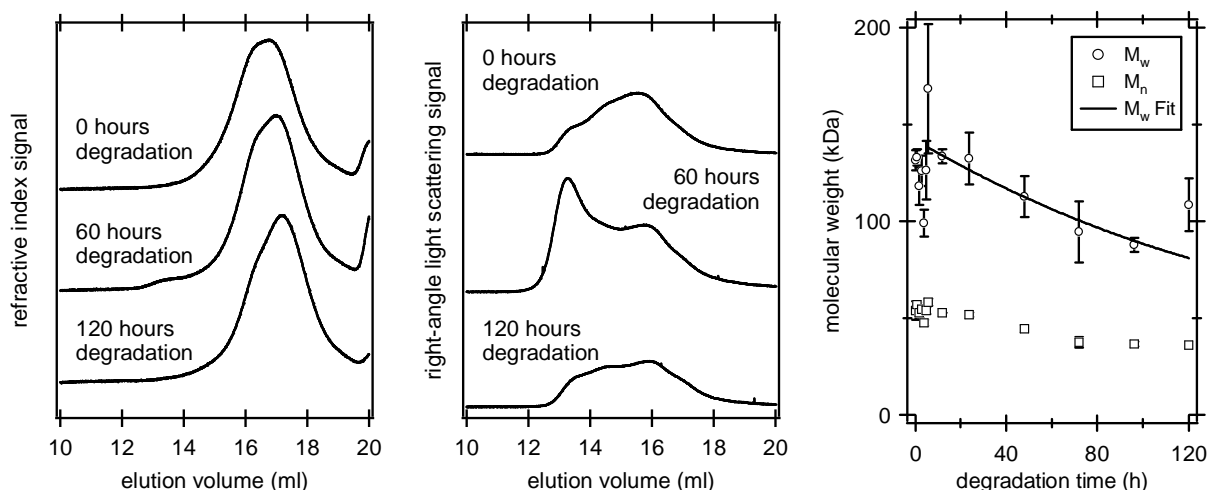
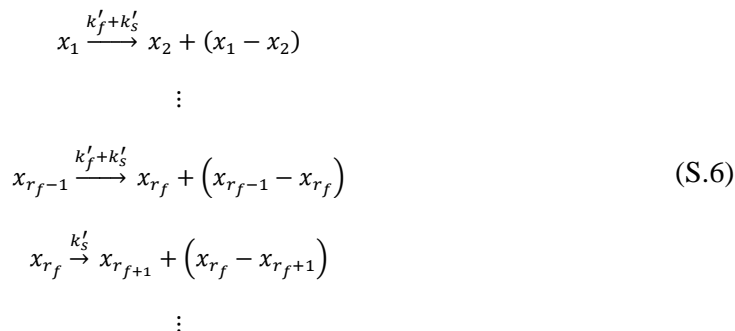


**Figure S9** (Left) Refractive index and (Center) right-angle light scattering detector signals for dextran-cysteamine-SNO sample at 0, 60, and 120 hours of degradation. (Right)  $M_w$  and  $M_n$  data as functions of time. The  $M_w$  data from 6 h to 120 h were fit to equation 3 with MWD moments obtained assuming a single coefficient,  $k'_s$ , and the initial  $M_w$  as adjustable parameters. The value of  $r_s = 4$  was fixed. Uncertainties represent the standard deviations of three measurements.

shown on the right in Fig. S7 with  $k'_s$  and  $M_w(t = 0)$  used as fit parameters. As discussed in the main text, the model does not account for some features, most notably, the rapid increase in molecular weight during the first 6 hours.

For the dextran-cysteine and dextran-cysteamine, a single rate coefficient was not sufficient to describe the degradation kinetics. We have modified the model of McCoy and Madras to include a fast and slow rate coefficient,  $k'_f$  and  $k'_s$ . These might correspond to the rates of hydrolysis of un-modified and modified regions of the dextran polymer chains. Correspondingly, the number of chain scissions per polymer chain by the fast hydrolysis is  $r_f - 1$  and the number of chain scissions per polymer chain by the slow hydrolysis is  $r_s - 1$ , with  $r_s > r_f$ . The reaction scheme S.1 is rewritten to reflect the fast and slow hydrolysis rates



$$x_{r_s-1} \xrightarrow{k'_s} x_{r_s} + (x_{r_s-1} - x_{r_s})$$

By analogy to equations S.2, the time derivatives for the MWD moments can be written, integrated, and summed to give the moments of the total MWD. In the present work, the degradation of the dextran-cysteine was modelled using  $r_f = 2$  and  $r_s = 3$ . The time derivatives for the moments of the MWDs for the reactant and product polymers are

$$\begin{aligned} \frac{dp_1^{(n)}}{dt} &= -(k'_f + k'_s)p_1^{(n)} \\ \frac{dp_2^{(n)}}{dt} &= -k'_s p_2^{(n)} + 2Z_n(k'_f + k'_s)p_1^{(n)} \\ \frac{dp_3^{(n)}}{dt} &= 2Z_n k'_s p_2^{(n)} \end{aligned} \quad (\text{S.7})$$

Integrating these equations with the initial conditions S.3 and summing according to equation S.5 gives

$$p^{(n)} = p_0^{(n)} \left[ \left( 1 - 2Z_n K' + 4Z_n^2 \frac{k'_s}{k'_f} \right) e^{-(k'_f + k'_s)t} + 2Z_n K' (1 - 2Z_n) e^{-k'_s t} + 4Z_n \right] \quad (\text{S.8})$$

where  $K' = (k'_f + k'_s)/k'_f$ . Equation S.8 was used with equations 2 and 3 in the main text to produce the model fits shown in Fig. 7 of the main text. The  $M_w(t)$  data in Fig. 7 were first fit to obtain values for the rate coefficients, and these were then used to predict the  $M_n(t)$  data.

For the dextran-cysteamine degradation, the model was formulated with  $r_f = 3$  and  $r_s = 5$ , resulting in the following time derivatives of the MWD moments

$$\begin{aligned} \frac{dp_1^{(n)}}{dt} &= -(k'_f + k'_s)p_1^{(n)} \\ \frac{dp_2^{(n)}}{dt} &= -(k'_f + k'_s)p_2^{(n)} + 2Z_n(k'_f + k'_s)p_1^{(n)} \\ \frac{dp_3^{(n)}}{dt} &= -k'_s p_3^{(n)} + 2Z_n(k'_f + k'_s)p_2^{(n)} \end{aligned} \quad (\text{S.9})$$

Electronic Supplementary Information

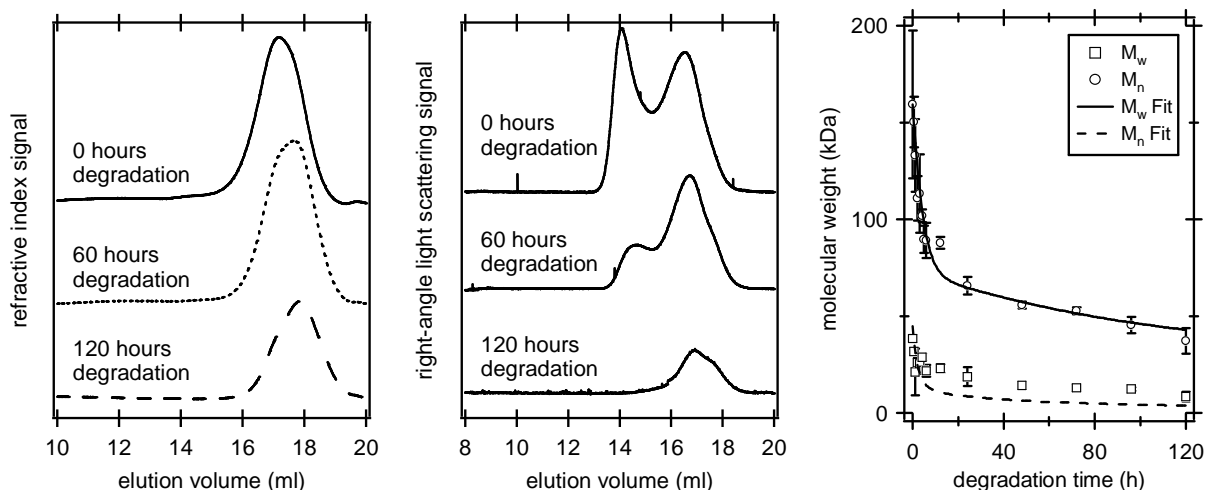


**Figure S10** (Left) Refractive index and (Center) right-angle light scattering detector signals for dextran-cysteamine sample at 0, 60, and 120 hours of degradation. (Right) The  $M_w$  and  $M_n$  data as functions of time. The  $M_w$  data were fit to equation 3 with MWD moments obtained assuming a fast and a slow rate coefficient  $k_f$  and  $k_s$  as the only adjustable parameters. The values of  $r_f = 3$  and  $r_s = 5$  were fixed. The “ $M_n$  fit” curve was predicted from equation (2) using the rate coefficients obtained from the fit to the  $M_w$  data. Uncertainties represent the standard deviations of three measurements.

$$\frac{dp_4^{(n)}}{dt} = -k'_s p_4^{(n)} + 2Z_n k'_s p_3^{(n)}$$

$$\frac{dp_5^{(n)}}{dt} = 2Z_n k'_s p_4^{(n)}$$

Equations S.9 can be integrated using the initial conditions S.3 and summed according to equation S.5 to give the following equation for the moments of the total MWD.

$$p^{(n)} = p_0^{(n)} \left\{ \left[ 1 + 2Z_n K' k'_f t - (2Z_n K')^2 (1 + k'_f t) + (2Z_n)^3 K'^2 \frac{k'_s}{k'_f} (2 + k'_f t) - (2Z_n)^4 \left( \frac{k'_s}{k'_f} \right)^2 (1 + 2K' + K' k'_f t) \right] e^{-(k'_f + k'_s)t} + \left[ (2Z_n K')^2 - (2Z_n)^3 K'^2 \frac{k'_s}{k'_f} (2 - k'_f t) + (2Z_n)^4 K'^2 (2K' - 3 - k'_s t) \right] e^{-k'_s t} + (2Z_n)^4 \right\} \quad (\text{S.10})$$

Equation S.10 was used along with equations 2 and 3 in the main text to produce the model fits shown in Figure S9. The  $M_w(t)$  data for the dextran-cysteamine degradation in Figure S9 were first fit to equation S.10 to obtain values for the rate coefficients, and these were then used to predict the  $M_n(t)$  data.



## References

1. Damodaran, V. B.; Joslin, J. M.; Wold, K. A.; Lantivit, S. M.; Reynolds, M. M. *J. Mater. Chem.* 2012, **22**, 5990.
2. McCoy, B. J.; Madras, G. *AIChE J.* 1997, **43**, 802.